Electron mobility degradation due to Remote Coulomb scattering in Ge MOSFET

Haoyu Xu, Jing Zhang, Shuhua Wei
Microelectronics Department, North China University of Technology
Beijing, China
jianwansannian@163.com (Haoyu Xu)

Xiaolei Wang, Wenwu Wang
Key Laboratory of Microelectronics Devices & Integrated Technology, Institute of Microelectronics,
Chinese Academy of Sciences
Beijing, China

***Abstract*—Remote Coulomb scatterings (RCS) on electron mobility degradation are experimentally investigated in Ge based metal-oxide-semiconductor field-effect-transistor (MOSFETs) with GeO_x/Al_2O_3 gate stacks. The mobility is found increased with thicker GeO_x (7.8-20.8 Å). The physical origin of this mobility dependence on GeO_x thickness is explored. The following factors are excluded: Coulomb scattering due to interfacial traps at GeO_x/Ge, phonon scattering, and surface roughness scattering. Therefore, the RCS from charges in gate stacks are studied. The charge distributions in GeO_x/Al_2O_3 gate stacks are experimentally evaluated. The bulk charges in Al_2O_3 and GeO_x are found negligible. The density of interfacial charge is $+3.2\times10^{12}$ cm^{-2} at GeO_x/Ge interface, and -2.3×10^{12} cm^{-2} at Al_2O_3/GeO_x interface. The electric dipole at Al_2O_3/GeO_x interface is found +0.15 V, corresponding to areal charge density of 1.9×10^{13} cm^{-2}. The origin of this mobility dependence on GeO_x thickness is attributed to the RCS due to electric dipole at Al_2O_3/GeO_x interface. And this remote dipole scattering is found to play a significant role on mobility degradation. The discovery of this new scattering mechanism indicates that engineering of Al_2O_3/GeO_x interface is key for mobility enhancement and device performance improvement. These results are helpful for understanding and engineering the Ge mobility enhancement.**

Keywords—Ge; Mobility; Remote Coulomb scatterings;

I. INTRODUCTION

Ge semiconductor is rather potential as channel material in order to further equivalently scale down the metal-oxide-semiconductor field-effect-transistors (MOSFETs) beyond 10 nm technology node.[1]-[5] For its successful application, a relevant parameter is effective channel mobility μ_{eff}, which is key point for Ge in replacement of Si substrate. The peak electron μ_{eff} is experimentally found to be ~750 $cm^2/V\cdot s$ using GeO_x passivation and Al_2O_3 barrier layer,[6], [7] which gate structure has been considered as one of the most feasible routes for realizing both low density of interfacial states (D_{it}) and low equivalent oxide thickness.[3], [4], [8], [9] Furthermore, to maximize the channel on-state current drivability, the scattering mechanisms that limit the μ_{eff} are of great concern. Developing a process technology that improves the mobility requires understanding the mechanism of Ge mobility degradation.[10] Several factors have been reported to induce mobility degradation, such as interfacial traps,[11], [12] surface roughness scattering,[7], [13] and oxygen atoms in Ge substrate.[14] However, the mechanisms of Ge mobility degradation are still not fully clear. Especially the remote Coulomb scatterings (RCS) from Ge gate stacks are not reported to data, even though the RCS is found to play an important role in Si based MOSFETs with high-k materials.[10], [15-18] In this paper, the RCS is experimentally investigated for Ge MOSFETs. The RCS from electric dipole at Al_2O_3/GeO_x interface is found to play a significant role on electron mobility degradation. This remote dipole scattering (RDS) indicates that the Al_2O_3/GeO_x interface is critical for device performance enhancement.

National Natural Science of China (No. 61176091)

II. EXPERIMENTAL

The Ge MOSFETs were fabricated as follows. The starting substrate is homemade 2 μm thick p-doped (100) epitaxial Ge on 8 inch p-doped (100) Si. The doping concentration is ~3×10^{17} cm^{-3} for epitaxial Ge. After the cleaning of Ge surface by 100:1 H_2O:HF for 60 s, the wafers were immediately capped with low temperature oxide SiO_2 (~80 Å). Then source/drain region was defined and phosphorus ions were implanted using an energy of 15 keV and a dose of 10^{15} cm^{-2}. The activation annealing was carried out at 600 °C for 1 min in N_2. Then the gate stacks were formed as follows. The gate region was opened by lithography-defined wet chemical etching, and the exposed Ge surface was again dipped in 100:1 H_2O:HF for 60 s. After that the Ge surface was immediately subjected to remote oxygen plasma oxidation to form GeO_x. Subsequently, Al_2O_3 was deposited by atomic layer deposition (ALD) using TMA and H_2O as precursors at 300° C. Then post deposition annealing (PDA) was performed at 400 ° C in N_2 for 5 min, followed by the ALD deposition of 3nm TiN and 75 nm W. After that, Ti source/drain contact and Al back contact were formed. Finally the wafers were subjected to the forming gas annealing at 400°C in 5% H_2/95% N_2 for 30 min. In addition, the MOS capacitors with $Ge/GeO_x/Al_2O_3$/TiN/W gate stacks were also fabricated with the same process conditions with Ge MOSFETs.

III. RESULTS AND DISCUSSION

A. Mobility for different GeO_x thicknesses

In order to investigate the remote Coulomb scattering, the mobility is evaluated as a function of the interfacial

GeO$_x$ thickness. Figure 1 shows the I_d-V_g characteristics of Ge nMOSFETs and electron mobility evaluated by the split capacitance-voltage (C-V) method at room temperature. Here four different thicknesses of GeO$_x$ interlayers were grown. From the Fig. 1(b), it can be seen that the mobility μ_{eff} at low inversion carrier density (N_s) increases with thicker GeO$_x$. The mobility in our experiments is lower than bulk Ge substrate, because of the crystal quality of the epitaxial Ge.[19] However, all the samples were fabricated using same epitaxial Ge. As a result, this mobility dependence on GeO$_x$ thickness is also available. It should be stated that the series resistance due to source/drain is experimentally determined to be negligible for 100 μm gate length (less than 3%), by using MOSFETs with different gate lengths (not shown here).

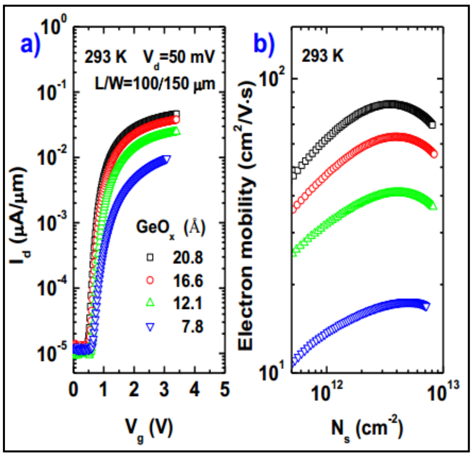

FIG. 1. (a) I_d-V_g of Ge nMOSFETs with Ge/GeO$_x$/Al_2O_3/TiN/W gate stacks at room temperature. The Al_2O_3 thickness is 10 nm. The GeO$_x$ thickness is given in the figure. (b) Electron mobility for different GeO$_x$ thicknesses.

B. Exclusion of D_{it} as origin

In order to understand this phenomenon, the D_{it} is firstly evaluated for the four samples. Fig. 2 shows the C-V curves of Ge/GeO$_x$/Al_2O_3/TiN/W MOS capacitors at 200 K and 100 K for 7.8 Å GeOx. The superior C-V characteristics are observed. Then the D_{it} are extracted by the low temperature conductance method for different GeO$_x$ thicknesses as shown in the Fig. 2(c). It can be seen that the D_{it} are nearly identical for different GeO$_x$ thicknesses. This is consistent with published reports that the D_{it} is nearly unchanged when GeO$_x$ thickness is larger than ~7 Å.[20], [21] Thus the D_{it} can be excluded as physical origin of mobility dependence on GeO$_x$ thickness.

C. Exclusion of remote phonon scattering as origin

Secondly the remote phonon scattering is considered. Fig. 3 shows the I_d-V_g characteristics and electron mobility at 77 K. It can be seen that the μ_{eff} still increases with thicker GeO$_x$. Considering that the phonon scattering can be ignored at 77 K,[22] the remote phonon scattering can also be ruled out.

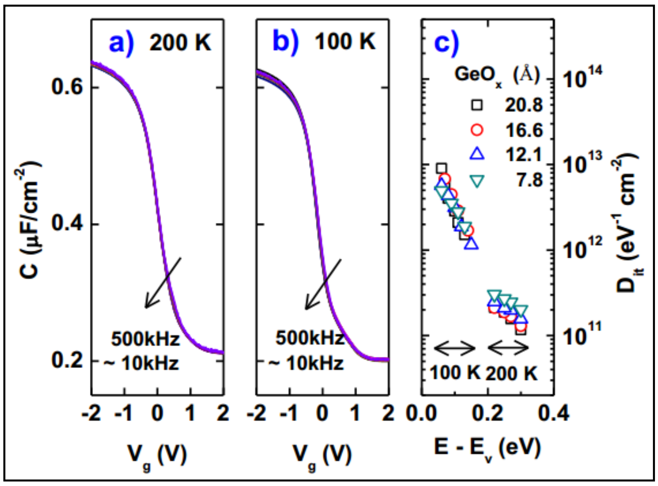

FIG. 2. C-V curves of Ge/GeO$_x$/Al_2O_3/TiN/W MOS capacitors at (a) 200 K and (b) 100 K for 7.8 Å GeO$_x$. The D_{it} is given in Fig. 2(c) for different GeO$_x$ thicknesses.

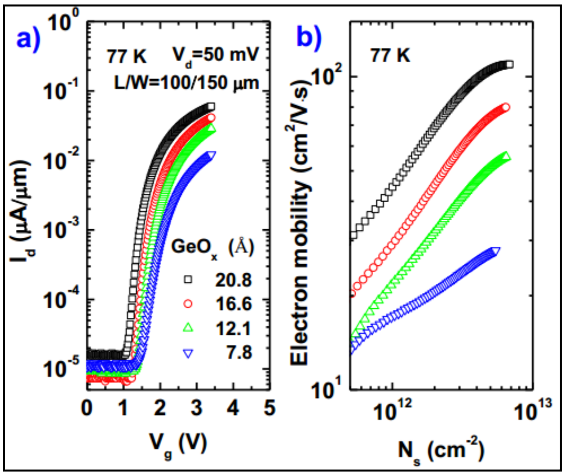

FIG. 3. (a) I_d-V_g and (b) electron mobility at 77 K.

D. Exclusion of surface roughness scattering as origin

Thirdly the surface roughness scattering is studied. The root mean square (rms) of surface roughness is experimentally determined to beidentical (~0.3 nm) for different GeO$_x$ thicknesses by atomic force microscope (AFM) (not shown here). Furthermore, the μ_{eff} at low N_s is mainly due to the Coulomb scattering but not surface roughness scattering.[23] Consequently, the surface roughness scattering cannot account for this mobility dependence on GeO$_x$ thickness.

E. Charge distribution in GeO$_x$/Al_2O_3 gate stacks

Based on the above discussion, there is another scattering mechanism, and we consider the RCS as the possible origin. In order to further investigate the RCS, the charge distribution in the Al_2O_3/GeO$_x$/Ge gate stacks is necessary to obtain. In our previous work, we experimentally extracted the charge distribution in Si gate stacks with high-k dielectric.[24] Similarly, the charge distribution in the Al_2O_3/GeO$_x$/Ge gate stacks can be extracted as follows. The flatband voltage (V_{FB}) of

TiN/Al_2O_3/terraced-GeO_x/Ge MOS capacitor is given as[24], [25]

$$V_{FB} = -\frac{Q_1}{\varepsilon_0\varepsilon_r}EOT - \frac{\varepsilon_1\rho_1}{2\varepsilon_0\varepsilon_r^2}EOT^2 - \frac{Q_2}{\varepsilon_0\varepsilon_r}EOT_2 + \frac{(\varepsilon_1\rho_1 - \varepsilon_2\rho_2)}{2\varepsilon_0\varepsilon_r^2}EOT_2^2 + \Delta + \varphi_{ms} \quad (1)$$

where Q_1 and Q_2 are areal charge densities at GeO_x/Ge and Al_2O_3/GeO_x interfaces, respectively. The ρ_1 and ρ_2 are bulk charge densities in GeO_x and Al_2O_3, respectively. The ε_0, ε_r, ε_1 and ε_2 are vacuum permittivity, relative permittivities of SiO_2, GeO_x and Al_2O_3, respectively. The EOT is equivalent oxide thickness of whole gate stacks, and EOT2 is equivalent oxide thickness of Al_2O_3 dielectric. The Δ is V_{FB} shift due to electric dipole at Al_2O_3/GeO_x interface. A positive dipole is defined when positive charges appear at Al_2O_3 side and equivalent negative charges at GeO_x side. The Φ_{ms} is the vacuum workfunction difference between TiN and Ge substrate. The Eq. (1) shows that the V_{FB} is a quadratic function of EOT. And the Q_1 and ρ_1 can be extracted from the linear and quadratic terms of V_{FB} vs. EOT plot. Fig. 4(a) shows the V_{FB}-EOT plot of TiN/10nm-Al_2O_3/terraced-GeO_x/Ge MOS capacitors at room temperature. It can be seen that a well linear fitting is obtained for V_{FB}-EOT curve. Then the interfacial charges at GeO_x/Ge interface (Q_1) can be determined to be $+3.2\times10^{12}$ cm^{-2}. And the bulk charges in GeO_x (ρ_1) can be negligible, indicating well quality of GeO_x by plasma oxidation. The ε_1 is calculated to be 5.1 from Fig. 4(b), which is consistent with the reported results.[26]

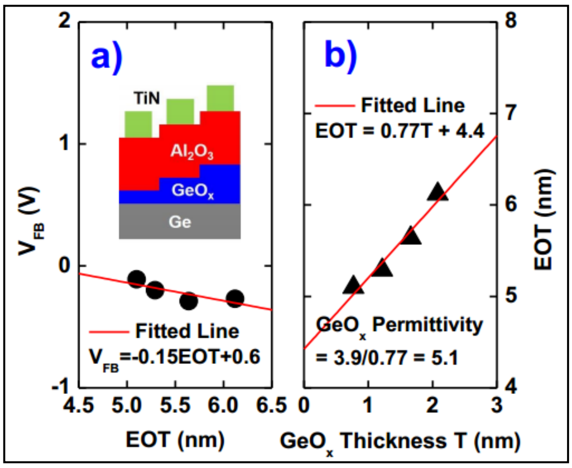

FIG. 4. (a) V_{FB} vs. EOT plot of TiN/10nm-Al_2O_3/terraced-GeO_x/Ge MOS capacitors at 500 kHz. (b) EOT vs. GeO_x thickness of TiN/10nm-Al_2O_3/terraced-GeO_x/Ge MOS capacitors.

In addition, The V_{FB} of TiN/terraced-Al_2O_3/GeO_x/Ge MOS capacitor is given as[24]

$$V_{FB} = -\frac{Q_1+Q_2}{\varepsilon_0\varepsilon_r}EOT + \frac{\varepsilon_2\rho_2 EOT_1}{\varepsilon_0\varepsilon_r^2}EOT - \frac{\varepsilon_2\rho_2}{2\varepsilon_0\varepsilon_r^2}EOT^2 + \frac{Q_2 EOT_1}{\varepsilon_0\varepsilon_r} - \frac{\varepsilon_2\rho_2}{2\varepsilon_0\varepsilon_r^2}EOT_1^2 + \Delta + \varphi_{ms} \quad (2)$$

here the EOT_1 is equivalent oxide thickness of GeO_x. Fig. 5(a) shows the V_{FB}-EOT plot of TiN/terraced-Al_2O_3/20.8Å-GeO_x/Ge MOS capacitors at room temperature.

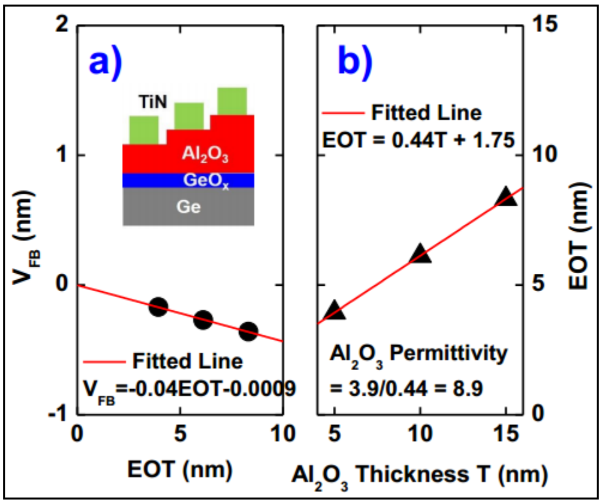

FIG. 5. (a) V_{FB} vs. EOT plot of TiN/terraced-Al_2O_3/20.8Å-GeO_x/Ge MOS capacitors at 500 kHz. (b) EOT vs. Al_2O_3 thickness of TiN/terraced-Al_2O_3/20.8Å-GeO_x/Ge MOS capacitors.

It can be seen that the a well linear fitted line can be obtained. Comparing the fitting result with the Eq. (2), the bulk charges ρ_2 in ALD Al_2O_3 can be determined to be 0 cm_{-3}. From the linear term in Eq. (2), the interfacial charges at Al_2O_3/GeO_x interface (Q_2) can be determined to be -2.3×10^{12} cm^{-2}.The ε_2 is calculated to be 8.9 from Fig. 5(b). The dipole Δ is evaluated as follows. From Eq. (2) the intercept of V_{FB}-EOT plot is given as

$$Intercept = \frac{Q_2 EOT_1}{\varepsilon_0\varepsilon_r} + \Delta + \varphi_{ms} \quad (3)$$

Then the Δ can be obtained if the intercept, EOT_1 and Φ_{ms} are known. The intercept is -0.0009 V from the Fig. 5(a). The EOT_1 is 1.75 nm from the intercept of EOT vs. Al_2O_3 thickness in Fig. 5(b). The vacuum workfunction of TiN has been experimentally determined to be 4.75 eV from TiN/terraced-SiO_2/Si MOS capacitors (not shown here). Considering the doping concentration in Ge substrate in our experiments, the Φ_{ms} can be calculated to be 0.03 eV. Then the interfacial dipole at Al_2O_3/GeO_x interface can be determined to be +0.15 eV. Next, the charge density Q_Δ that induces this dipole is estimated. The dipole Δ can be expressed based on Gauss theorem

$$\Delta = \frac{Q_\Delta T_\Delta}{\varepsilon_0\varepsilon_\Delta} \quad (4)$$

The T_Δ is inner distance between positive and negative charges of dipole, and is taken as ~0.3 nm.[27], [28] The ε_Δ is relative permittivity of the inner gap in dipole, and is taken as $2\varepsilon_1\varepsilon_2/(\varepsilon_1+\varepsilon_1)=2\times5.7\times8.9/(5.7+8.9)=6.95$.[27],[28] Then charge density Q_Δ is calculated to be 1.9×10^{13} cm^{-2}, which is about one order of magnitude larger than the interfacial charges (Q_2) at Al_2O_3/GeO_x interface.

F. Remote dipole scattering

The remote Coulomb scattering is discussed. Based on the above results,three types of charges appear in the $Al_2O_3/GeO_x/Ge$ gate stacks: interfacial charges at GeO_x/Ge interface (Q_1), interfacial charges at Al_2O_3/GeO_x interface (Q_2), and electric dipole at Al_2O_3/GeO_x interface (Δ). The Q_1 cannot account for the mobility dependence on GeO_x thickness in Fig. 1(b) and 3(b), because the scattering rate due to Q_1 is identical for different GeO_x thicknesses. The RCS due to Q_2 can be negligible compared with RCS due to the Δ, because the Q_2 is one order of magnitude smaller than Q_Δ. Furthermore, the scattering rate due to RDS changes as $\exp(-2k_F t_{IL})$ with interfacial GeO_x thickness t_{IL},[29], [30] where k_F is the Fermi wavenumber of the inversion electrons. Therefore, we can conclude that RDS is responsible for the mobility degradation with decreasing the GeO_x thickness. Considering the exponential dependence of RDS on interlayer GeO_x thickness, the RDS is a significant contribution of the mobility degradation in the ultrathin EOT region. From Fig. 1(b), the enhancement factor of peak mobility of 20.8 Å nm GeO_x against the 12.1 Å GeOx is around 2. Fig. 6 schematically shows the scattering mechanisms for electron mobility. The RDS significantly reduces the mobility. Therefore, reduction or even elimination of this interfacial dipole should enable us to improve the electron mobility.

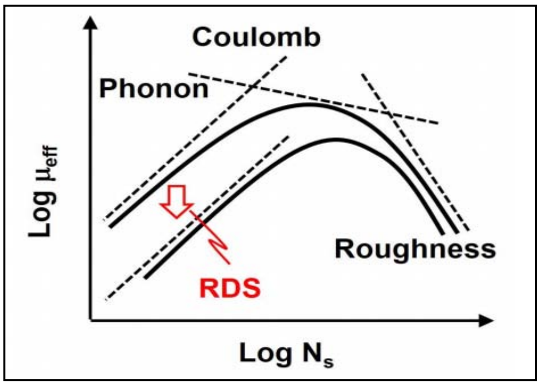

FIG. 6. Schematic of the RDS on electron mobility.

IV.CONCLUSIONS

In summary, the RCS for mobility degradation of Ge nMOSFET is experimentally investigated, and the electric dipole at Al_2O_3/GeO_x interface plays a significant role on mobility degradation. Our findings indicate that understanding of the interface dipole at Al_2O_3/GeO_x is critically important for mobility analysis. Engineering of this interface is a key for both mobility improvement and V_{FB} tuning. The discovery of this new scattering mechanism in Ge based MOSFETs is helpful for further improvement of mobility and device performance.

ACKNOWLEDGEMENTS

This work was financially supported by National Natural Science Foundation of China (Nos. 61504163, 61574168, 61504001) and the Beijing Municipal Natural Science Foundation (No.4162023).

REFERENCES

[1] S. Ogawa et al., J Applied Physics 118 (23), 235704 (2015).
[2] C. Lu et al., Applied Physics Letters 107(7), 072904 (2015).
[3] T. Hosoi et al., Applied Physics Letters 107(25), 252104 (2015).
[4] R. Asahara et al., Applied Physics Letters 106 (23), 233503(2015).
[5] T. Kanashima et al., J Applied Physics 118 (22), 225302 (2015).
[6] C. H. Lee et al., presented at the Symposium on VLSI Technology, 2013, p.28.
[7] R. Zhang et al., presented at the Symposium onVLSI Technology, 2013, p.26.
[8] R. Zhang et al., Applied Physics Letters 98 (11), 112902 (2011).
[9] Y. X. Zheng et al., IEEE Electron Device Letters, 36 (9), 881-883(2015).
[10] S.-i. Saito et al., J Applied Physics 98 (11), 113706 (2005).
[11] 11.D. Kuzum et al., IEEE Transactions on Electron Devices 58 (1),59-66 (2011).
[12] R. Zhang et al., IEEE Transactions on Electron Devices 60 (3), 927-934 (2013).
[13] C. H. Lee et al., presented at the Symposium on VLSI Technology, 2014, p.1.
[14] C. H. Lee et al., presented at the IEEE International Electron Devices Meeting, 2014, p.32.5.1.
[15] Y. Nian et al., IEEE Transactions on Electron Devices, 47 (2), 440-447 (2000).
[16] S. Barraud et al., J Applied Physics 104 (7), 073725 (2008).
[17] D. Casterman and M. M. De Souza, Journal of Applied Physics 107 (6), 063706 (2010).
[18] D. Esseni and A. Abramo, IEEE Transactions on Electron Devices, 50(7), 1665-1674 (2003).
[19] X. Yu et al., Microelectronic Engineering 147, 196-200 (2015).
[20] R. Zhang et al., IEEE Transactions on Electron Devices 59 (2), 335-341 (2012).
[21] X. Wang et al., Applied Surface Science 357, Part B, 1857-1862 (2015).
[22] N. Taoka et al., Journal of Applied Physics 108 (10), 104511 (2010).
[23] S. Takagi et al., IEEE Transactions on Electron Devices 41 (12), 2357-2362 (1994).
[24] X. Wang et al., Applied Physics Letters 97 (6), 062901 (2010).
[25] S. Deng et al., Journal of The Electrochemical Society 155 (2), G33-G38 (2008).
[26] 27. W. Monch, Semiconductor Surfaces and Interfaces, Springer, p. 92(2001).
[27] 28. S. G. Louie et al., Physical Review B 15(4), 2154-2162 (1977).
[28] 29. D. Jena et al., Journal of Applied Physics 88(8), 4734-4738 (2000).
[29] 30. H. Ota et al., presented at the IEEE International Electron Devices Meeting, 2007, p.6.